Cell Stress and Chaperones (2024) 29:272–284
https://doi.org/10.1016/j.cstres.2024.03.004

Roles of heat shock protein A12A in the development of diabetic cardiomyopathy

Yunxiao Jia[a] · Yunhao Yu[a] · Chenxi Gao[a] · Yuehua Li[b] · Chuanfu Li[c] · Zhengnian Ding[d] · Qiuyue Kong[d,*] · Li Liu[a,b,*]

Received: 7 December 2023 / Revised: 8 February 2024 / Accepted: 9 March 2024

Abstract

Long-term hyperglycemia can lead to diabetic cardiomyopathy (DCM), a main lethal complication of diabetes. However, the mechanisms underlying DCM development have not been fully elucidated. Heat shock protein A12A (HSPA12A) is the atypic member of the Heat shock 70kDa protein family. In the present study, we found that the expression of HSPA12A was upregulated in the hearts of mice with streptozotocin-induced diabetes, while ablation of HSPA12A improved cardiac systolic and diastolic dysfunction and increased cumulative survival of diabetic mice. An increased expression of HSPA12A was also found in H9c2 cardiac cells following treatment with high glucose (HG), while overexpression of HSPA12A-enhanced the HG-induced cardiac cell death, as reflected by higher levels of propidium iodide cells, lactate dehydrogenase leakage, and caspase 3 cleavage. Moreover, the HG-induced increase of oxidative stress, as indicated by dihydroethidium staining, was exaggerated by HSPA12A overexpression. Further studies demonstrated that the HG-induced increases of protein kinase B and forkhead box transcription factors 1 phosphorylation were diminished by HSPA12A overexpression, while pharmacologically inhibition of protein kinase B further enhanced the HG-induced lactate dehydrogenase leakage in HSPA12A overexpressed cardiac cells. Together, the results suggest that hyperglycemia upregulated HSPA12A expression in cardiac cells, by which induced cell death to promote DCM development. Targeting HSPA12A may serve as a potential approach for DCM management.

Keywords Heat shock protein A12A (HSPA12A) · Diabetic cardiomyopathy (DCM) · Cardiac cell injury · High glucose · AKT/FOXO1 signaling

Introduction

Diabetes is a metabolic disorder characterized by hyperglycemia. With its high morbidity (1 in 11 adults in the world), diabetes has become a serious public health problem.[1,2] Diabetic cardiomyopathy (DCM) is a specific cardiac manifestation of patients with diabetes and shows a negative impact on the prognosis in affected patients. However, the effective approach for DCM treatment is still lacking, partially due to that the exact mechanisms underlying DCM development have not been fully understood.[2,3]

DCM is characterized by left ventricular hypertrophy and diastolic dysfunction in the early phase up to overt heart failure with reduced systolic function in the advanced stages.[4-6] Although multiple factors have been shown to be involved in DCM pathogenesis, hyperglycemia is considered to play a central role in DCM development.[7] By

* Qiuyue Kong
kongqiuyue@njmu.edu.cn

* Li Liu
liuli@njmu.edu.cn

[a] Department of Geriatrics, First Affiliated Hospital of Nanjing Medical University, Nanjing, Jiangsu Province, China

[b] Key Laboratory of Targeted Intervention of Cardiovascular Disease, Collaborative Innovation Center for Cardiovascular Disease Translational Medicine, Nanjing Medical University, Nanjing, Jiangsu Province, China

[c] Departments of Surgery, East Tennessee State University, Johnson City, TN, USA

[d] Department of Anesthesiology, The First Affiliated Hospital of Nanjing Medical University, Nanjing, Jiangsu Province, China.

Published online: 12 March 2024

promoting excessive generation of reactive oxygen species (ROS) and other products such as advanced glycation end products, hyperglycemia directly disrupts cardiomyocyte homeostasis to induce cell death.[7] Considering that cardiomyocyte death is not only a pathological character but also a prominent contributor to DCM development, improving cardiomyocyte survival upon hyperglycemia challenge therefore represents a promising therapeutic approach for DCM management.

Studies demonstrate the involvement of protein kinase B (Akt)/Forkhead box transcription factors 1 (FoxO1) signaling in hyperglycemia-evoked cell death.[8-11] As a transcription factor, FoxO1 promotes apoptotic signaling by inducing the expression of multiple proapoptotic members when FOXO1 localizes in nuclei. The nuclear localization and activation of FOXO1 are regulated by post-translational modifications such as phosphorylation.[11,12] Evidence demonstrated that Akt is a kinase for FOXO1 phosphorylation, leading to FOXO1 exported from nuclei, and ultimately inhibiting the apoptotic process.[9,11,12]

Heat shock protein A12A (HSPA12A), an atypical member of the heat shock protein 70 family, shows ubiquitous expression in different organs including the heart.[13,14] We have recently reported that HSPA12A promotes the development of obesity and non-alcoholic fatty liver disease.[14,15] We also have demonstrated that HSPA12A protects the liver during endotoxemia and inhibits metastasis of renal cancer.[16,17] Specifically, we have shown that HSPA12A protects against ischemic stroke in an Akt-dependent manner.[18] It is possible, therefore, that HSPA12A may play a role in DCM development by modulating the Akt/FOXO1-mediated cardiomyocyte death.

To test this possibility, we examined the effects of HSPA12A on streptozotocin (STZ)-induced DCM and high glucose (HG)-induced cardiomyocyte death using both mouse and cell culture models. We found that HSPA12A expression was upregulated in mouse DCM hearts, while ablation of HSPA12A attenuated DCM development. Further studies revealed that upregulation of HSPA12A promoted HG-induced cardiac cell death through modulating Akt/FOXO1 signaling. The findings suggest that targeting HSPA12A in cardiomyocytes has therapeutic potential for the management of DCM in patients.

Results

HSPA12A expression is upregulated in the hearts of diabetic mice

To investigate the possible involvement of HSPA12A in DCM pathogenesis, we first examined the expression of HSPA12A in the hearts of diabetic mice. To this aim, diabetes was induced in mice by STZ administration (Figure 1(a)). Blood glucose increased significantly 3 days after STZ administration, and the hyperglycemia was maintained throughout experiments ($P < 0.01$, Figure 1(b)). After diabetes was induced for 12 weeks, cardiac diastolic function was examined using echocardiography. As shown in Figure 1(c) ($P < 0.01$), diabetes for 12 weeks decreased the E/A ratio compared to the vehicle-treated control mice, indicating that DCM was developed following hyperglycemia for 12 weeks. Meanwhile, a higher expression of HSPA12A was detected in DCM hearts ($P < 0.01$, Figure 1(d)).

Ablation of HSPA12A does not affect hyperglycemia but improves the survival of diabetic mice

The upregulation of HSPA12A in DCM hearts motivated us to investigate the role of HSPA12A in DCM pathogenesis. To this aim, HSPA12A knockout (*Hspa12a*$^{-/-}$) mice and their wild-type (WT) littermates were employed in the experiments (Figure 2(a)). HSPA12A showed no expression in hearts of *Hspa12a*$^{-/-}$ mice (Figure 2(b)). Blood glucose increased significantly after STZ administration in both genotypes ($P < 0.01$, Figure 2(c)), but the level of hyperglycemia was not different between *Hspa12a*$^{-/-}$ mice and WT mice ($P > 0.05$, Figure 2(c)). However, *Hspa12a*$^{-/-}$ mice displayed higher cumulative survival than WT mice after STZ-induced diabetes ($P < 0.05$, Figure 2(d)). Together, the data indicate that the improved survival in diabetic *Hspa12a*$^{-/-}$ mice was not mediated by limiting hyperglycemia.

Ablation of HSPA12A attenuates cardiac dysfunction and cardiac hypertrophy in diabetic mice

Considering that DCM is a main lethal complication of diabetes, we thus examined cardiac performance in *Hspa12a*$^{-/-}$ mice and their WT controls. Echocardiographic examination demonstrated that following STZ-induced diabetes for 12 weeks, cardiac ejection fraction (EF%) and fraction shortening (FS%) were decreased in both genotypes, when compared to their vehicle controls ($P < 0.01$, Figure 3(a) and Table 1). However, the diabetes-induced decreases of EF% and FS% were attenuated in *Hspa12a*$^{-/-}$ mice compared to WT controls ($P < 0.05$, $P < 0.01$, Figure 3(a) and Table 1), suggesting that HSPA12A ablation attenuated cardiac systolic dysfunction in diabetic mice. Similar results were found in the examination of cardiac diastolic function, which showed that following STZ-induced diabetes for 12 weeks, the E/A ratio was decreased in both genotypes, but this decrease

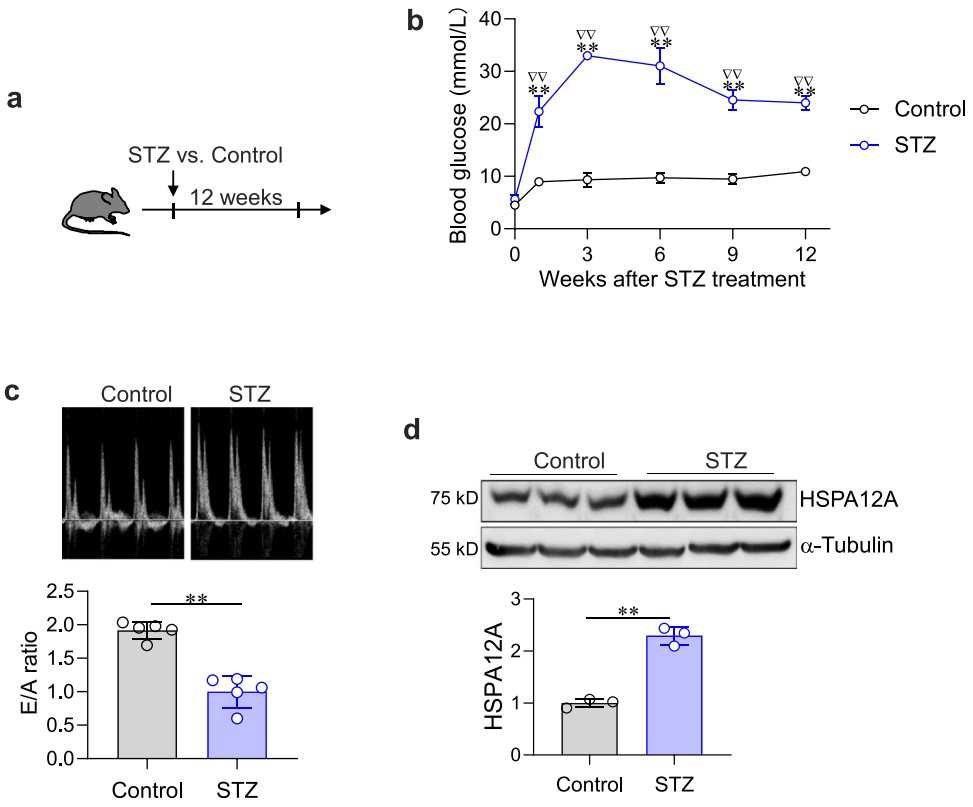

Fig. 1 HSPA12A expression was upregulated in DCM hearts. (a) Mouse experimental setting. (b) Levels of blood glucose were measured after treatment with STZ or vehicle control. $^{**}P < 0.01$ vs. base level ("0" time point) of the same treatment, $^{\nabla\nabla}P < 0.01$ vs. same time point of the control group. n = 3/group. (c) Cardiac diastolic function was measured using echocardiography at 12 weeks after STZ treatment. The diastolic function was expressed as the ratio of E-wave and A-wave, which was derived by measuring flow velocities across the mitral valve using pulsed Doppler. The upper panel shows the representative Doppler images. $^{**}P < 0.01$. n = 5/group. (d) HSPA12A expression in hearts was analyzed at 12 weeks after STZ treatment using immunoblotting analysis. The blots against α-Tubulin served as loading controls. $^{**}P < 0.01$. n = 3/group. Abbreviations used: A, A peak; DCM, diabetic cardiomyopathy; E, E peak; STZ, streptozotocin.

was attenuated in *Hspa12a*$^{-/-}$ mice compared to WT controls ($P < 0.01$, Figure 3(b) and Table 1).

Cardiac hypertrophy is another characteristic of DCM besides cardiac dysfunction.[6] Following STZ-induced diabetes for 12 weeks, heart weight was significantly increased in both genotypes when compared to their vehicle controls, while this increase of heart weight was attenuated in *Hspa12a*$^{-/-}$ mice compared to WT controls ($P < 0.05$ or $P < 0.01$, Figure 3(c)). In line with this, the diabetes-induced increase of cardiomyocyte size was attenuated in *Hspa12a*$^{-/-}$ mice compared to WT mice ($P < 0.05$ or $P < 0.01$, Figure 3(d)). Taken together, the data suggest that ablation of HSPA12A protects the heart against DCM development.

HSPA12A expression is upregulated in cardiac cells upon higher glucose challenge

Cardiomyocyte injury plays a pivotal role in DCM development.[19] We thus investigated whether HSPA12A is involved in hyperglycemia-induced cardiac cell death. To this aim, *in vitro* experiments were performed using H9c2 cardiac cells (Figure 4(a)). Exposure to HG-induced injury in H9c2 cardiac cells, as reflected by increases in abnormal cellular morphology, lactate dehydrogenase (LDH) leakage, and propidium iodide (PI) staining compared to control cells ($P < 0.01$, Figure 4(b–d)). Meanwhile, when HG-induced injury of H9c2 cardiac cells, HSPA12A expression was also upregulated following HG exposure ($P < 0.01$, Figure 4(e)). The results suggest that HSPA12A may play a role in HG-induced cardiac cell injury.

Overexpression of HSPA12A aggravates the HG-induced cardiac cell injury

To evaluate the direct role of HSPA12A on the HG-induced cardiac cell injury, we overexpressed HSPA12A (*Hspa12a*$^{O/E}$) in H9c2 cardiac cells by infection with HSPA12A-adenovirus, and the empty adenovirus-infected H9c2 cardiac cells served as negative controls (NC) (Figure 5(a)). Treatment of HG for 24 h increased

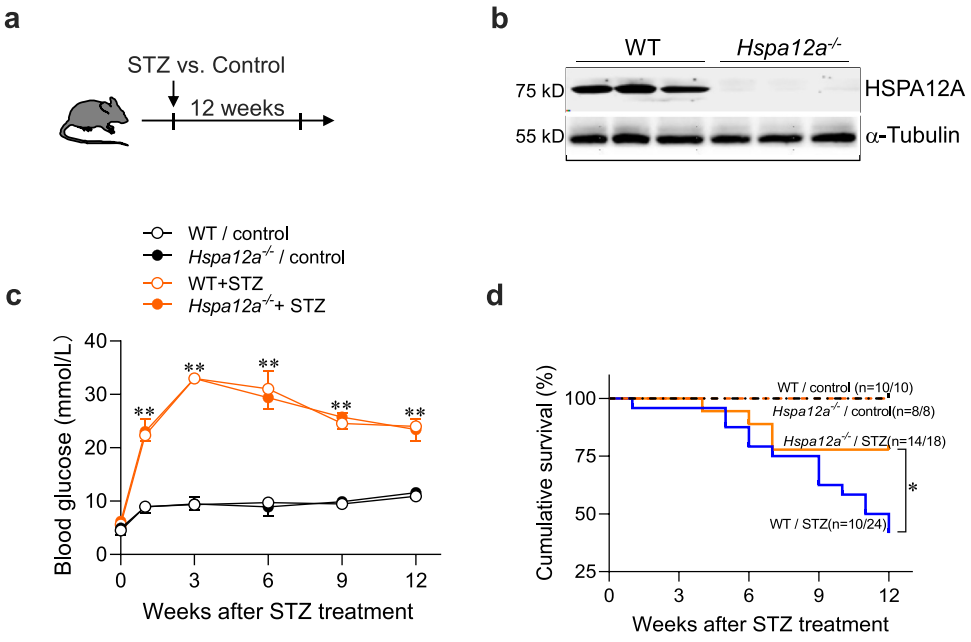

Fig. 2 Ablation of HSPA12A improved survival of diabetic mice. (a) Mouse experimental setting. (b) Expression of HSPA12A in the hearts of WT and *Hspa12a*$^{-/-}$ mice was compared using immunoblotting. The blots against α-Tubulin served as loading controls. Note that HSPA12A showed no expression in the hearts of *Hspa12a*$^{-/-}$ mice. n = 10/group. (c) Levels of blood glucose were measured using tail vein blood. Note that blood glucose was not different between STZ-treated WT and *Hspa12a*$^{-/-}$ mice. $^{**}P < 0.01$ vs. the same time point and same genotype group without STZ treatment. n = 3/group. (d) Mouse survival was recorded after STZ treatment. $^{**}P < 0.05$. n = 10 for control WT group, n = 8 for control *Hspa12a*$^{-/-}$ group, n = 24 for STZ-WT group, n = 18 for STZ-*Hspa12a*$^{-/-}$ group. Abbreviations used: *Hspa12a*$^{-/-}$ mice, *Hspa12a* knockout mice; STZ, streptozotocin; WT, wild-type.

LDH leakage in both NC and *Hspa12a*$^{O/E}$ groups when compared to their control groups. However, the HG-induced LDH leakage was greater in *Hspa12a*$^{O/E}$ group than in NC group ($P < 0.01$, Figure 5(b)). Similarly, the HG-induced increase of PI-stained cells was also enhanced in *Hspa12a*$^{O/E}$ group than in NC groups ($P < 0.01$, Figure 5(c)). In supporting these results, the HG-induced cleavage of caspase 3 was exaggerated in *Hspa12a*$^{O/E}$ H9c2 cells compared to NC controls ($P < 0.05$ or $P < 0.01$, Figure 5(d)). Altogether, the results indicate that overexpression of HSPA12A aggravated the HG-induced cardiac cell injury.

Overexpression of HSPA12A aggravates the HG-induced oxidative stress in cardiac cells

Evidence demonstrates that hyperglycemia causes oxidative stress to promote cardiac cell injury.[20] We, therefore, measured the effect of HSPA12A on HG-induced generation of ROS in H9c2 cardiac cells using a dihydroethidium (DHE) fluorescence probe. As shown in Figure 6(a) ($P < 0.05$ or $P < 0.01$), HG increased DHE fluorescence intensity in both NC and *Hspa12a*$^{O/E}$ groups. However, the HG-induced increase of DHE fluorescence intensity was greater in *Hspa12a*$^{O/E}$ group than in the NC group. Heme oxygenase-1 (HO-1) is an enzyme that has antioxidant properties.[21] Unexpectedly, *Hspa12a*$^{O/E}$ group displayed higher levels of HO-1 expression either at the basal level or following HG treatment ($P < 0.05$ or $P < 0.01$, Figure 6(b)).

Overexpression of HSPA12A inhibits the HG-induced phosphorylation of Akt and FOXO1in cardiac cells

Studies demonstrate that cell death can be promoted by activation of forkhead box 1 (FOXO1), while the activity of FOXO1 is suppressed following their phosphorylation by Akt.[12] Considering that we have previously shown a regulatory effect of HSPA12A on Akt phosphorylation in brain,[18] we investigated whether Akt may play a role in the regulation of HSPA12A in HG-induced cardiac cell death. As shown in Figure 7 ($P < 0.01$), HG increased phosphorylation levels of Akt and FOXO1 in NC groups but not in *Hspa12a*$^{O/E}$ group. Moreover, following HG treatment, *Hspa12a*$^{O/E}$ group showed lower levels of Akt and FOXO1 phosphorylation than the NC groups ($P < 0.01$, Figure 7).

Inhibition of Akt exacerbates the HSPA12A-enhanced injury of HG-treated cardiac cells

To clarify the role of reduced Akt phosphorylation in the HSPA12A-enhanced injury of HG-treated cardiac cells, we treated *Hspa12a*$^{O/E}$ H9c2 cardiac cells with an

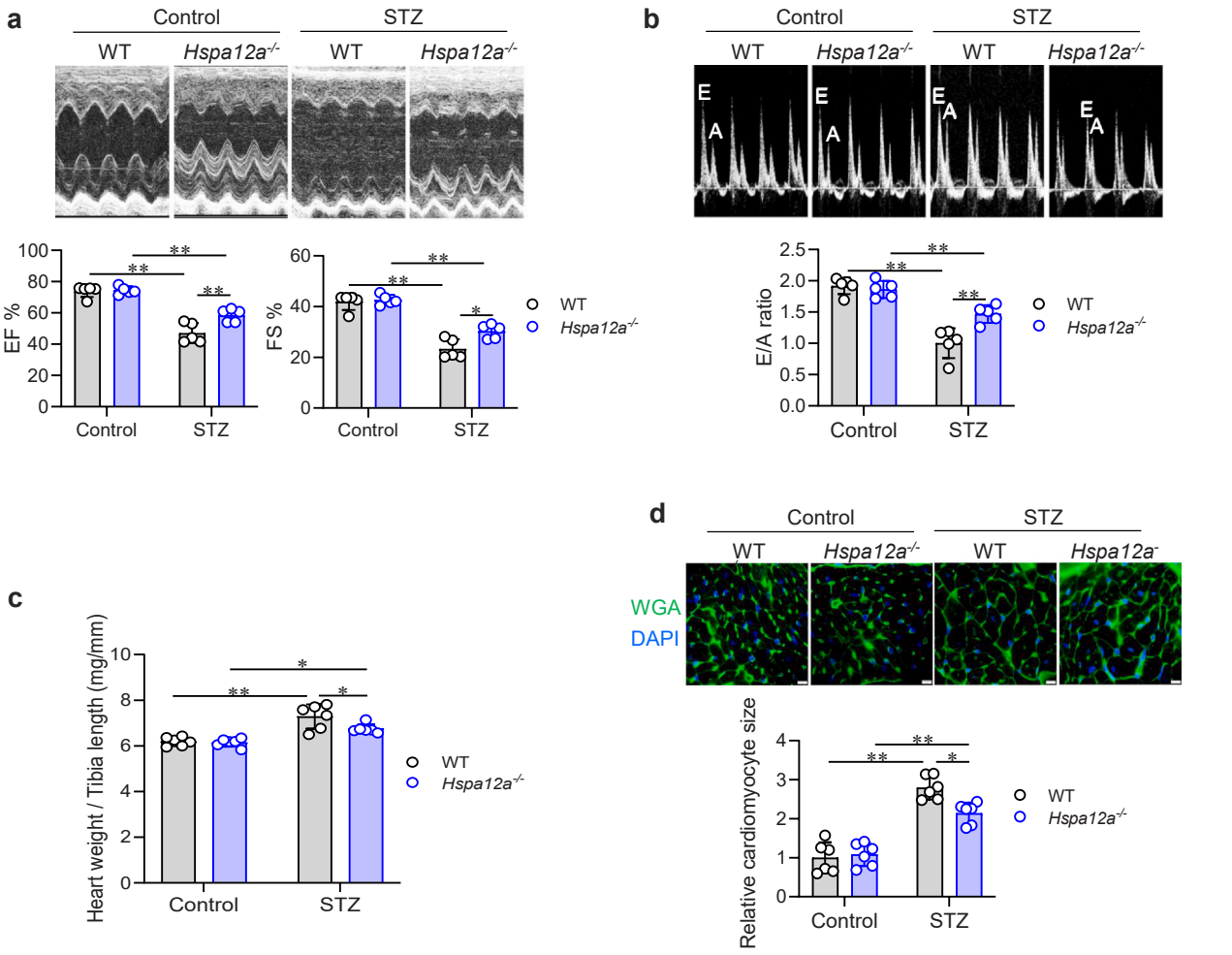

Fig. 3 Ablation of HSPA12A attenuated cardiac dysfunction in diabetic mice. (a) Cardiac systolic function was examined at 12 weeks after STZ administration using echocardiography. The upper panel shows the representative M-mode images. $^{**}P < 0.01$ and $^{*}P < 0.05$, n = 5/group. (b) Cardiac diastolic function was examined after STZ administration for 12 weeks using echocardiography. The upper panel shows the representative pulse Doppler images. $^{**}P < 0.01$, n = 5/group. (c) Heart weight was examined 12 weeks after STZ administration and expressed as the ratio of heart weight to tibia length (mg/mm). $^{**}P < 0.01$ and $^{*}P < 0.05$, n = 6/group. (d) The size of cardiomyocytes was examined at 12 weeks after STZ administration using WGA staining on the cardiac frozen section. DAPI was to counterstain nuclei. Scale bar = 10 μm. $^{**}P < 0.01$ and $^{*}P < 0.05$, n = 6/group. Abbreviations used: *Hspa12a*$^{-/-}$ mice, *Hspa12a knockout* mice; STZ, streptozotocin; WGA, wheat germ agglutinin; WT; wild-type. DAPI:4', 6-diamino-2-phenylindole.

Akt inhibitor MK-2206. MK-2206 significantly decreased Akt phosphorylation levels in *Hspa12a*$^{O/E}$ H9c2 cardiac cells ($P < 0.01$, Figure 8(a)). Notably, inhibition of Akt phosphorylation with MK-2206 further enhanced the HG-induced LDH leakage of *Hspa12a*$^{O/E}$ cardiac cells ($P < 0.01$, Figure 8(b)), suggesting that HSPA12A promoted the HG-induced cardiac cell injury through inhibition of Akt phosphorylation.

Discussion

The main finding of this study is that HSPA12A was upregulated in the DCM heart, while ablation of HSPA12A in mice attenuated the STZ-induced DCM and mortality of mice. Further experiments demonstrated that upregulation of HSPA12A promoted HG-evoked cardiac cell death through modulating Akt/FOXO1 signaling.

DCM is a diabetes-induced pathophysiological condition that is characterized by cardiac hypertrophy and cardiac dysfunction and can eventually result in heart failure.[4] The prevalence of DCM is high, ranging from 19 to 26% in diabetic patients.[4] Because DCM is not only a cause of death but also a risk factor for coronary diseases in DCM patients,[22] the management of DCM is therefore critical for improving the prognosis of the affected patient. Studies demonstrate that some of the heat shock proteins (HSPs) are involved in the pathogenesis of DCM. HSPs are highly conserved chaperones

Table 1
Echocardiographic measurements.

Group n = 5	WT	*Hspa12a*$^{-/-}$	WT + STZ	*Hspa12a*$^{-/-}$ + STZ
A, mm/s	247.64 ± 39.95	249.94 ± 45.73	355.34 ± 111.78	202.28 ± 50.69
E, mm/s	473.66 ± 77.04	459.79 ± 58.11	333.74 ± 53.57[a]	291.02 ± 53.82[b]
E/A	1.92 ± 0.12	1.86 ± 0.12	1 ± 0.21[c]	1.47 ± 0.13[b]
LVVs, μL	12.28 ± 2.62	15.94 ± 4	36.24 ± 11.88[c]	22.07 ± 4.51
LVVd, μL	47.36 ± 10.45	61.29 ± 10.9	68.58 ± 12.49	52.84 ± 8.12
EF%	73.87 ± 3.37	74.34 ± 2.22	47.01 ± 5.72[c]	58.48 ± 3.74[b]
FS%	41.92 ± 2.9	42.59 ± 1.8	23.24 ± 3.49[c]	30.27 ± 2.52[b]
LVIDs, mm	1.96 ± 0.17	2.24 ± 0.3	3 ± 0.43[c]	2.48 ± 0.19
LVIDd, mm	3.38 ± 0.31	3.8 ± 0.32	3.92 ± 0.56	3.55 ± 0.22
Body weight, g	29.93 ± 1.56	30.29 ± 1.55	25.02 ± 0.96[c]	25.89 ± 1.23[b]

Abbreviations used: A, A peak; E, E peak; EF%, ejection fraction %; FS%, fractional shortening %; LVIDd, LV end-systolic dimension; LVIDs, LV end-diastolic dimension; LVVd, left ventricular end-diastolic volume; LVVs, LV end-systolic volume; STZ, streptozotocin; WT, wild-type; Standard Error of Mean.
Data presented as mean ± SEM.
[a]$P < 0.05$ compared to WT.
[b]$P < 0.01$ compared to *Hspa12a*$^{-/-}$.
[c]$P < 0.01$ compared to WT.

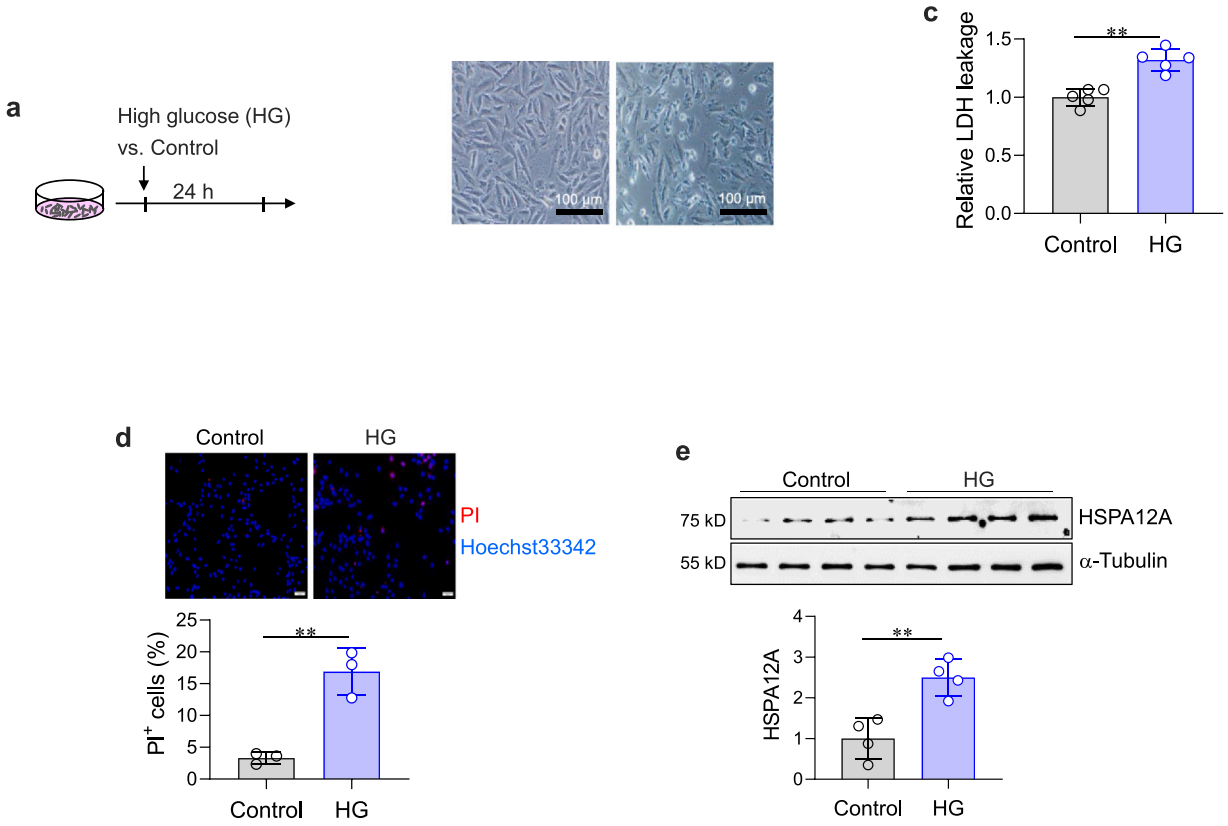

Fig. 4 HSPA12A expression was upregulated in HG-treated cardiac cells. (a) Cardiac cell experimental setting. (b) Cell morphology. Scale bar = 100 μM. n = 3/group. (c) LDH leakage was examined 24 h after HG exposure by examining LDH activity in a culture medium of H9c2 cardiac cells. $^{**}P < 0.01$, n = 5/group. (d) PI staining was performed in H9c2 cardiac cells 24 h after HG exposure. Scale bar = 100 μm. $^{**}P < 0.01$, n = 3/group. (e) HSPA12A expression in H9c2 cardiac cells 24 h after HG treatment using immunoblotting analysis. The blots against α-Tubulin served as loading controls. $^{**}P < 0.01$. n = 4/group. Abbreviations used: HG, high glucose; LDH, lactate dehydrogenase; PI, propidium iodide.

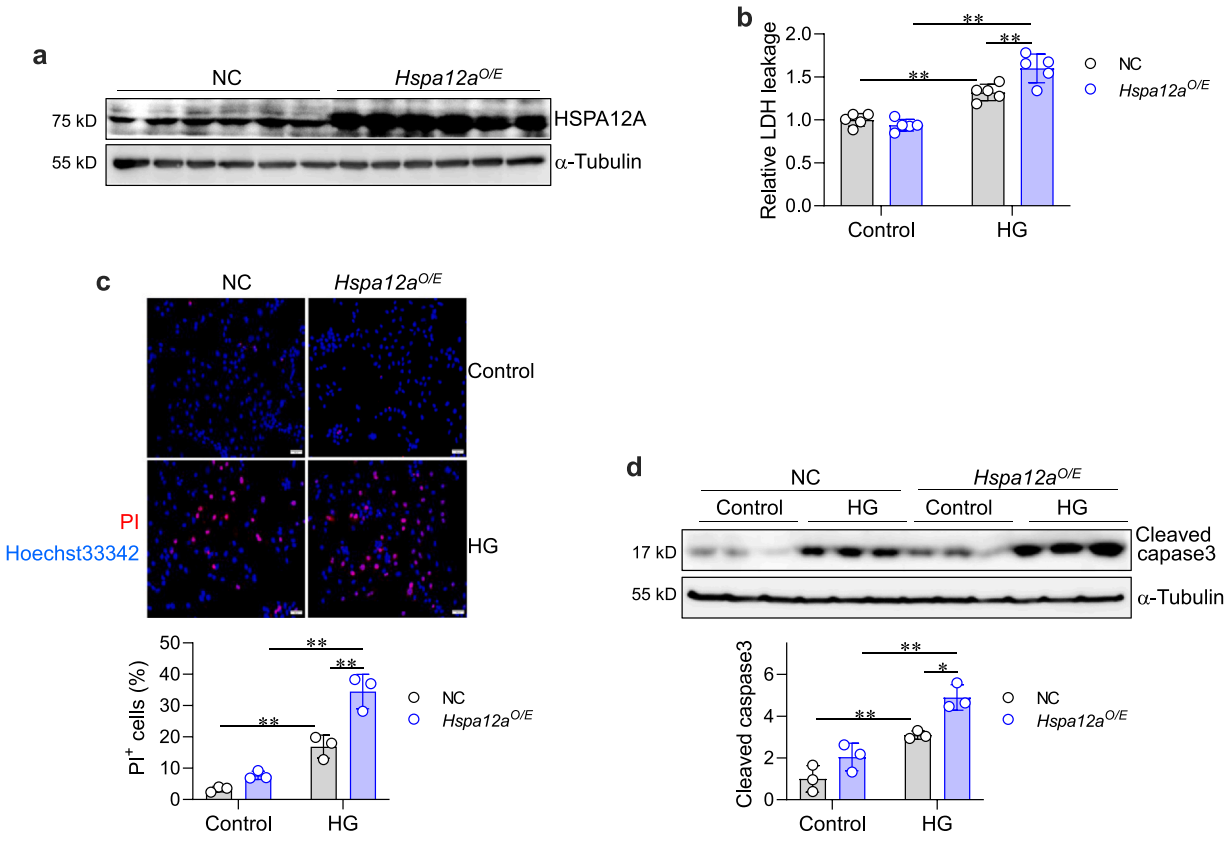

Fig. 5 HSPA12A overexpression enhanced the HG-induced injury of cardiac cells. (a) HSPA12A was overexpressed in H9c2 cardiac cells by infection with *Hspa12a*-adenovirus (*Hspa12a*$^{O/E}$). The H9c2 cardiac cells infected with empty adenovirus served as NCs. (b) LDH leakage was examined 24 h after HG exposure by examining LDH activity in a culture medium of H9c2 cardiac cells. $^{**}P < 0.01$, n = 5/group. (c) PI staining was performed in H9c2 cardiac cells 24 h after HG exposure. $^{**}P < 0.01$, n = 3/group. (d) Cleavage of caspase 3 was examined 24 h after HG treatment using immunoblotting analysis. The blots against α-Tubulin served as loading controls. $^{**}P < 0.01$ and $^{*}P < 0.05$, n = 3/group. Abbreviations used: HG, high glucose; *Hspa12a*$^{O/E}$, HSPA12A overexpression; LDH, lactate dehydrogenase; NC, negative controls; PI, propidium iodide.

among species and are divided into several families based on their molecular weight. Among them, HSP27, HSP72, and HSP60 show protective roles against DCM.[23-26] However, the non-successful clinical translation of these HSPs in DMC treatment encourages us to investigate whether other HSPs may play roles in DCM pathogenesis. HSPA12A was initially identified in mice by Han and his colleagues[13] in 2003. By blasting HSPA12A against the National Center for Biotechnology Information database, they grouped HSPA12A into the Heat shock 70kDa protein family because HSPA12A contains the ATPase domain of the Heat shock 70kDa protein family. However, the ATPase domain in HSPA12A was separated in two parts by spacer amino acids 245–311, thus HSPA12A was considered an atypical member of the Heat shock 70kDa protein family. When taken into account that HSPA12A expression is altered by certain stimuli in humans, rodents, and oysters,[13,14,27] the changes of HSPA12A expression by stimulation is a conserved stress response. In this study, we found that HSPA12A expression was upregulated in the DCM heart of mice, while ablation of HSPA12A in mice attenuated cardiac diastolic and systolic dysfunction, alleviated cardiomyocyte hypertrophy, and improved animal survival in STZ-induced diabetic mice. In different with the protective roles of other HSPs mentioned above, our findings revealed that the upregulation of HSPA12A promoted the development of DCM. Also, we found that STZ increased cardiomyocyte size nearly 3-fold but only increased heart weight to 115%. This could be partially due to that long-term exposure to hyperglycemia results in changes in cell population, cell size, cell death, and cell phenotype in the heart.

Considering that we found an upregulation of HSPA12A in DCM hearts whereas HSPA12A attenuated cardiac dysfunction and improved mice survival in STZ-induced diabetic mice, we performed *in vitro* experiments to investigate whether upregulated HSPA12A impacts cardiac cell injury upon hyperglycemia exposure. We found that HG increased HSPA12A expression and induced death of cardiac cells, and

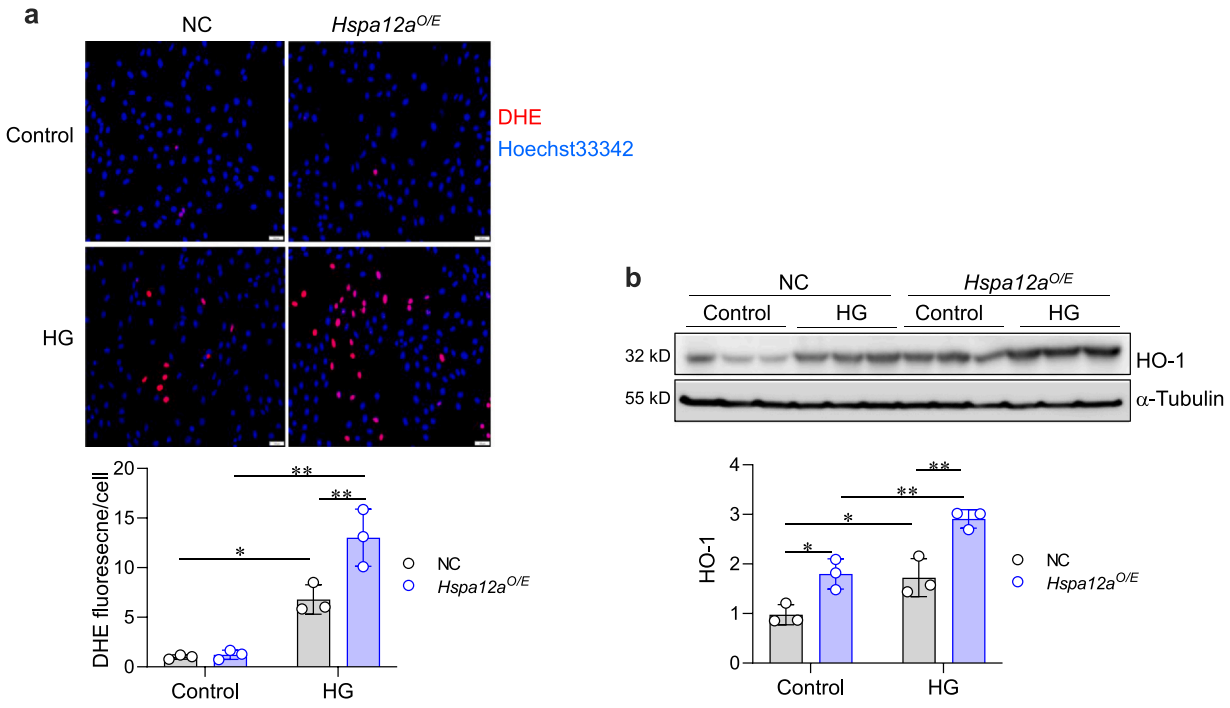

Fig. 6 HSPA12A overexpression enhanced the HG-induced oxidative stress in cardiac cells. (a) DHE staining was performed in H9c2 cardiac cells 24 h after HG exposure. $^{**}P < 0.01$ and $^{*}P < 0.05$, n = 3/group. (b) HO-1 expression was examined 24 h after HG treatment using immunoblotting analysis. The blots against α-Tubulin served as loading controls. $^{**}P < 0.01$ and $^{*}P < 0.05$, n = 3/group. Abbreviations used: DHE, dihydroethidium; *Hspa12a*$^{O/E}$, HSPA12A overexpression; HG, high glucose; NC, negative controls.

overexpression of HSPA12A further exaggerated the HG-evoked ROS production and cardiac cell injury. However, HSPA12A increased the antioxidant HO-1 expression, suggesting that the upregulation of HO-1 might be an adaptive response to the greater oxidative stress. The findings indicate a role of HSPA12A in the medication of hyperglycemia-induced injury of cardiac cells.

In this study, we used an STZ-inducted type 1 diabetic mouse model. DCM is the main cardiac complication of both type 1 and type 2 diabetes.[28-30] Various animal models of type 1 and type 2 diabetes have been developed to investigate the pathological mechanisms of DCM. Among them, the STZ-induced type 1 diabetic mouse model mimics the various perturbations observed in diabetic myocardium, including glucose oxidation, oxidative stress, lipotoxicity, cell death, fibrosis, and contractile function and size. Also, cardiac remodeling and cardiac dysfunction were severe in STZ-induced type 1 diabetic mouse models. Interestingly, type 1 diabetic mice showed higher cardiomyocyte size (hypertrophy) compared with T2 diabetic mice.[31] Therefore, STZ-induced type 1 diabetes in mice is a proven and widely accepted model to study the pathogenesis of diabetes and its complications.

Evidence has demonstrated an involvement of Akt/FOXO1 signaling in the pathogenesis of diabetic complications, including DCM.[32,33] FOXO1 is one of four mammalian isoforms of the FOXO transcription factor family. When localizing in the nucleus, FOXO1 has the ability to regulate the transcription of its target genes including the proapoptotic genes. Cytosolic FOXO1 is considered inactive. Studies demonstrate that following phosphorylated by Akt, the phosphor-FOXO1 shuttled to the cytoplasm to be inactivated. In this study, we found that when overexpression of HSPA12A-enhanced the HG-induced cardiac cell death, HSPA12A overexpression also suppressed phosphorylation levels of Akt and FOXO1 upon HG exposure. Moreover, inhibition of Akt further exaggerated the HSPA12A overexpression-induced increase of cell injury following HG exposure. Together, the findings indicate that HSPA12A promoted cardiac cell injury through, at least in part, modulating the Akt/FOXO1 signaling.

In conclusion, hyperglycemia upregulated HSPA12A expression to promote the development of DCM through increasing cardiac cell death. Targeting HSPA12A expression has the therapeutic potential for DCM management.

Materials and methods

Chemicals and antibodies

D-glucose (DG), glucose oxidase (GO), wheat germ agglutinin (WGA), and DHE were purchased from Sigma-

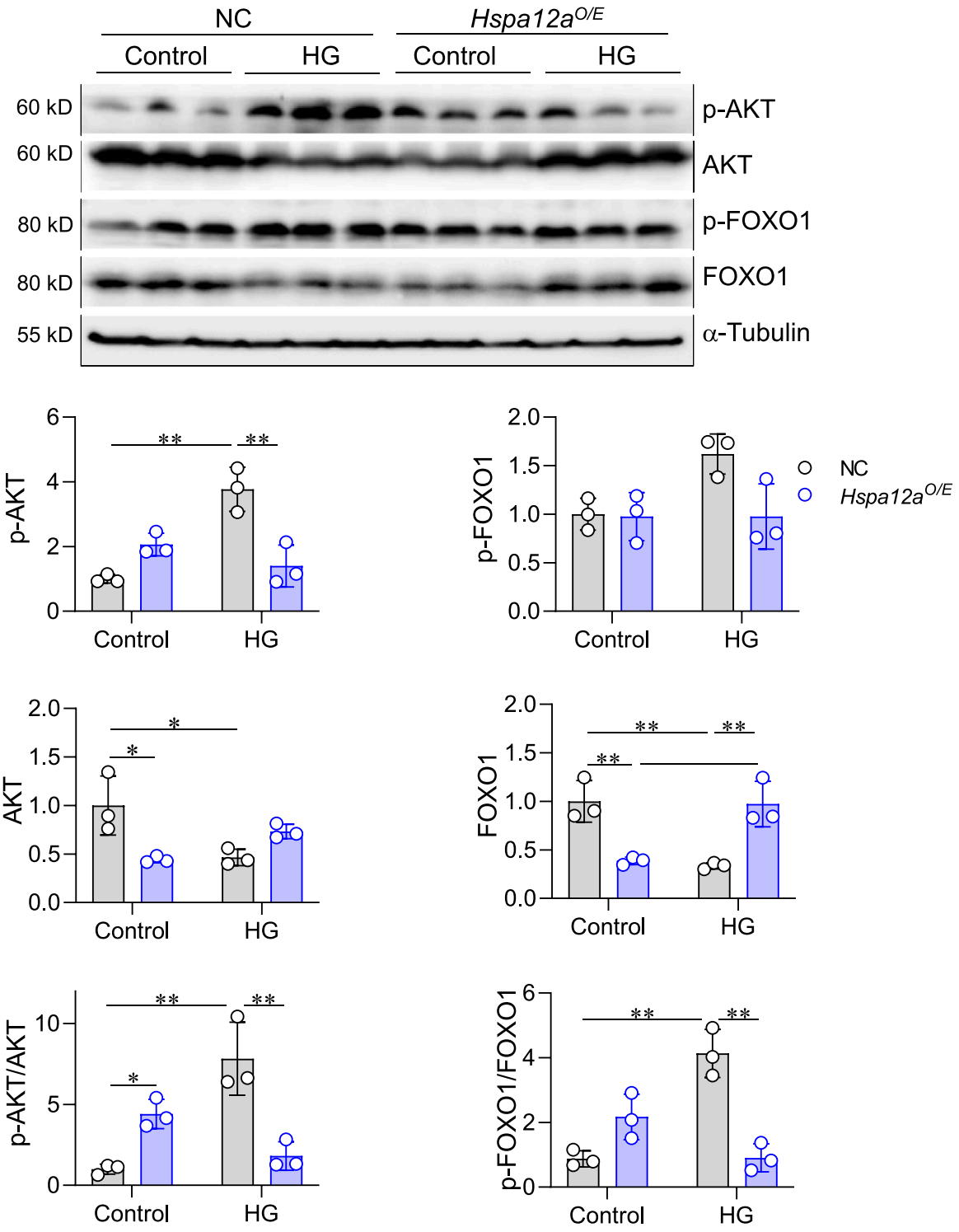

Fig. 7 Effects of HSPA12A on phosphorylation levels of Akt and FOXO1. H9c2 cardiac cells were challenged with HG for 24 h. Cells were harvested for the immunoblotting against the indicated antibodies. $^{**}P < 0.01$ and $^{*}P < 0.05$, n = 3/group. Abbreviations used: Akt, protein kinase B; FOXO1, forkhead box transcription factors 1; HG, high glucose; NC, negative controls.

Aldrich (St. Louis, MO). The LDH assay kit was from Solarbio (Beijing, China). PI was from Beyotime Biotechnology (Shanghai, China). Hoechst33342 reagent was obtained from Invitrogen (Carlsbad, CA). 4', 6-diamino-2-phenylindole reagent was from Cell Signaling Technology (Boston, MA). The Bicinchoninic Acid Assay protein assay kit was obtained from Pierce (Rockford, IL). The primary antibody for HSPA12A was

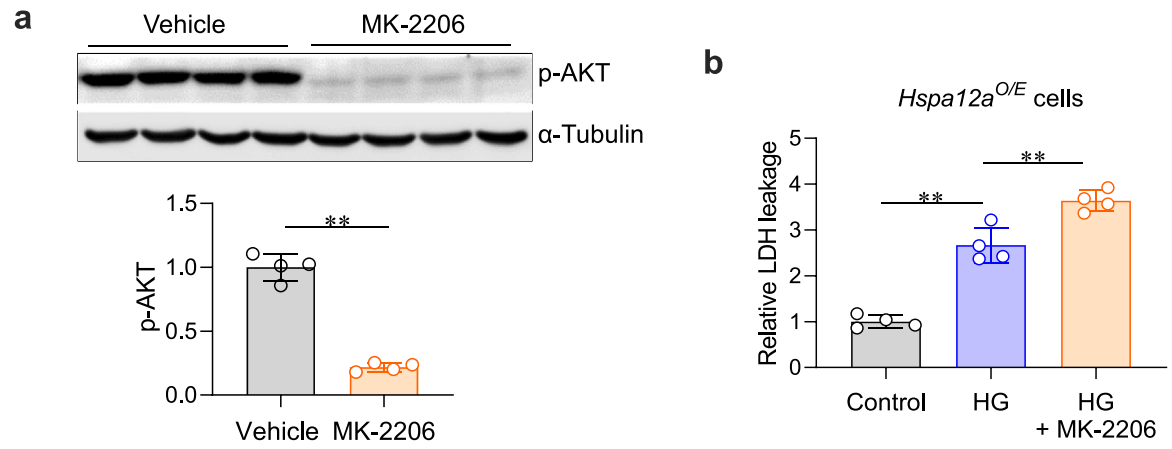

Fig. 8 Effects of Akt inhibition on injury of the HG-treated *Hspa12a*$^{O/E}$ cardiac cells. *Hspa12a*$^{O/E}$ H9c2 cardiac cells were challenged with HG for 24 h in the presence or absence of Akt inhibitor MK-2206. LDH leakage was examined by evaluating LDH activity in a culture medium of H9c2 cardiac cells. $^{**}P < 0.01$, n = 4/group. Abbreviations used: Akt, protein kinase B; HG, high glucose; *Hspa12a*$^{O/E}$, HSPA12A overexpression; LDH, lactate dehydrogenase.

from Abcam (Cambridge, MA). Primary antibodies for Akt, phosphor-Akt, FOXO1, phosphor-FOXO1, and Cleaved-caspase3 were from Cell Signaling Technology (Beverly, MA). The primary antibody for HO-1 was from Proteintech (Chicago, CA). Anti-α-Tubulin antibody was from Sigma-Aldrich. MK-2206 was from MedChemExpress (Monmouth Junction, NJ). Bovine serum albumin was from Roche (Basel, Switzerland). Dulbecco's Modified Eagle's medium and fetal bovine serum were from Gibco (Shelton, CT). High-sig enhanced chemiluminescence western blotting substrate was from Tanon (Shanghai, China). STZ was from Biosharp (Hefei, China).

Generation of HSPA12A knockout (*Hspa12a*$^{-/-}$) mice

Hspa12a$^{-/-}$ mice were generated using the Cre-locus of X-overP1 recombinant system as previously described.[14,18] Briefly, the region of the *Hspa12a* gene containing exons 2–4 was retrieved from a 129/sv Bicinchoninic Acid Assay clone (Bacterial artificial chromosome/PAC Resources Center, Oakland, CA) using a retrieval vector containing two homologous arms. Exons 2 and 3 were replaced by locus of X-overP1 sites flanking a Mouse phosphoglycerate kinase 1 promoter-neo cassette as a positive selection marker. To remove the *Hspa12a* gene, the chimeric mice were crossed with EIIa-Cre transgenic mice.

The mice were bred at the Model Animal Research Center of Nanjing University and were maintained in the Animal Laboratory Resource Facility of the same institution. All experiments conformed to the Guide for the Care and Use of Laboratory Animals published by the US National Institutes of Health (NIH Publication, 8th Edition, 2011) and international guidelines on the ethical use of animals. The animal care and experimental protocols were under the regulation and approval of the Committee on Animal Care of Nanjing University and Nanjing Medical University.

Induction of DCM in mice

To induce diabetes, 8–10 weeks-old male mice were administrated with a single dosage of STZ (120 mg/kg, soluble in citric acid buffer, pH 4.5) through intraperitoneal injection according to the previous method.[34] The control mice were injected with the same volume of citric acid buffer (vehicle). Blood glucose levels were measured using mouse tail vein blood from day 3 after STZ administration, and then blood glucose was monitored weekly up to 12 weeks after STZ treatment. Mice were considered to be diabetic and enrolled in the study only if they had hyperglycemia (> 16.7 mmol/L). Mice were randomly allocated to each experimental group. For tissue collection, mice were sacrificed by overdose anesthesia with pentobarbital sodium (150 mg/kg, intraperitoneal injection) and cervical dislocation.

Mortality of mice

Hspa12a$^{-/-}$ mice and WT mice were randomly assigned into vehicle control and STZ treatment groups. For STZ groups, mice received a single injection of STZ (120 mg/kg, intraperitoneally). For vehicle control groups, mice were injected with the same volume of citrate buffer. The survival of mice was recorded twice a day until the end of the experiment (a total of 12 weeks). The numbers for each group were as follows: n = 10 for the WT/control group, n = 8 for *Hspa12a*$^{-/-}$/control group, n = 24 for WT/STZ group, n = 18 for *Hspa12a*$^{-/-}$/STZ group.

Echocardiography

Twelve weeks after STZ administration, the cardiac function of mice was examined by two-dimensional echocardiography using the Vevo770 system equipped with a 35-MHz transducer (Visualsonics, Toronto, Canada) according to our previous methods.[35,36] Briefly, after anaesthetized with inhalation of 1.5–2% isoflurane, mouse cardiac function was analyzed by an observer blinded to the treatment. The parameters were obtained in M-mode and pulsed Doppler tracings and averaged using 3–5 cardiac cycles. Each group contained five mice.

WGA staining

Cardiomyocyte size was evaluated using WGA staining according to our previous study.[37] Briefly, cardiac tissues were collected at the papillary muscle level after treatment with STZ for 12 weeks. After fixed, the cardiac tissues were prepared for frozen sections with 4 μm thick, followed by WGA (10 μg/mL) incubation for 30 min. DAPI was used to counterstain nuclei. The staining was photographed by fluorescence microscopy and quantified using Cellsens Dimention 1.15 software (Olympus, Tokyo, Japan). Each group contained six mice.

Heart weight

Mice were sacrificed by cervical dislocation after overdose anesthesia by pentobarbital sodium 150 mg/kg (intraperitoneal injection). After that, the hearts were harvested, washed in Phosphate-balanced solution to remove blood clots, wiped with paper, and weighed. Also, the tibia of the left hind limb of the mice was removed, and the length was measured. To exclude the confounding factor of mouse body size on heart weight, the heart mass was expressed as the ration of heart weight/tibia length (mg/mm). Each group contained six mice. The above information was incorporated in the revised manuscript.

Cell culture and treatment

Rat H9c2 cardiac cells were from the Type Culture Collection of the Chinese Academy of Sciences. Cells were maintained in Dulbecco's Modified Eagle's medium supplemented with 10% fetal bovine serum and 1% penicillin/streptomycin. To mimic a HG environment, H9c2 cardiac cells were treated with 33 mM of DG and 5 mU of GO according to previous studies.[38,39] The H9c2 cells that were treated with 5.5 mM of DG and 5 mU of GO served as controls. Analysis was performed 24 h after treatment. In the Akt inhibition experiments, cells were pretreated with an Akt inhibitor MK-2206 (3 μM) 30 min prior to the HG challenge.

Overexpression of HSPA12A

For gain-of-function experiments, H9c2 cardiac cells were infected with adenovirus (20 Multiple viral infection) that carry three flag-tagged *Hspa12a* expression sequences to overexpress HSPA12A. H9c2 cells infected with empty adenovirus served as NC.

Measurement of LDH leakage

LDH leakage is an indicator of cell injury. In our study, a culture medium was collected for measuring LDH activity 24 h after HG treatment using the assay kit according to the manufacturer's instructions. Each group contained five repeats.

Cell morphology

H9c2 cardiac cells were treated with 33 mM of DG and 5 mU of GO. The H9c2 cells that were treated with 5.5 mM of DG and 5 mU of GO served as controls. Bright field images of each group were taken with a phase-contrast microscope 24 h after treatment. Each group contained three repeats.

PI fluorescence staining

PI staining is an indicator of cell death. Twenty-four hours after HG treatment, cells were stained with PI (10 μg/mL) for 30 min. The staining was observed under a fluorescence microscope (Zeiss Ltd, Germany). Death cells were expressed as a percentage of PI-positive cells to total cells. More than three fields per sample were taken at random. Image acquisition and cell scoring were conducted by an investigator blinded to the treatment of experiments. Each group contained three repeats.

Measurement of intracellular ROS content

Intracellular ROS content was measured by DHE assay as described in our previous studies.[39] Briefly, after treatment with HG for 24 h, H9c2 cardiac cells were stained with DHE (10 μM) for 30 min. The staining was observed, and images were captured using a fluorescence microscope with a magnification of 10× (Zeiss Ltd.). The fluorescence intensity was quantified using Cellsens Dimention 1.15 software (Olympus). Each group contained three repeats.

Immunoblotting

Twenty-four hours after HG treatment, H9c2 cardiac cells were collected for immunoblotting analysis according to our previous methods.[14,15] Briefly, an equal amount of cellular protein extracts was separated by 10% Sodium dodecyl sulfate-polyacrylamide gel electrophoresis and then transferred onto polyvinylidene difluoride membranes (Millipore Corp., Bedford, MA). After being blocked in 5% skimmed milk for 1 h at room temperature, the membranes were probed with primary antibodies at 4 °C overnight followed by incubation with peroxidase-conjugated secondary antibodies. For loading control, the membranes were probed with anti-α-Tubulin. The signals were quantified by scanning densitometry and the results from each experimental group were expressed as relative integrated intensity compared with that of controls. Each group contained three repeats.

Statistical analysis

Data are expressed as the mean ± standard deviation. Groups were compared using Student's two-tailed unpaired t test, log-rank test, or using one-way and two-way Analysis of variance followed by Tukey's post-hoc test. A P value of < 0.05 was considered significant.

Data availability statement No data was used for the research described in the article.

Declarations of interest The authors declare that they have no known competing financial interests or personal relationships that could have appeared to influence the work reported in this paper.

Acknowledgments This work was supported by the National Natural Science Foundation of China (82170295, 82170851, 82002023, and 81970692) and a project funded by the Collaborative Innovation Center for Cardiovascular Disease Translational Medicine.

References

1. Zheng Y, Ley SH, Hu FB. Global aetiology and epidemiology of type 2 diabetes mellitus and its complications. *Nat Rev Endocrinol.* 2018;2:88–98. https://doi.org/10.1038/nrendo.2017.151
2. Xie S, Liu S, Zhang T, et al. USP28 serves as a key suppressor of mitochondrial morphofunctional defects and cardiac dysfunction in the diabetic heart. *Circulation.* 2024;149:684–706. https://doi.org/10.1161/circulationaha.123.065603
3. Murtaza G, Virk HUH, Khalid M, et al. Diabetic cardiomyopathy - a comprehensive updated review. *Prog Cardiovasc Dis.* 2019;4:315–326. https://doi.org/10.1016/j.pcad.2019.03.003
4. Dillmann WH. Diabetic cardiomyopathy. *Circ Res.* 2019;8:1160–1162. https://doi.org/10.1161/circresaha.118.314665
5. Paolillo S, Marsico F, Prastaro M, et al. Diabetic cardiomyopathy: definition, diagnosis, and therapeutic implications. *Heart Failure Clin.* 2019;3:341–347. https://doi.org/10.1016/j.hfc.2019.02.003
6. Tong M, Saito T, Zhai P, et al. Mitophagy is essential for maintaining cardiac function during high fat diet-induced diabetic cardiomyopathy. *Circ Res.* 2019;9:1360–1371. https://doi.org/10.1161/circresaha.118.314607
7. Jia G, Whaley-Connell A, Sowers J. Diabetic cardiomyopathy: a hyperglycaemia- and insulin-resistance-induced heart disease. *Diabetologia.* 2018;1:21–28. https://doi.org/10.1007/s00125-017-4390-4
8. Battiprolu PK, Gillette TG, Wang ZV, Lavandero S, Hill JA. Diabetic cardiomyopathy: mechanisms and therapeutic targets. *Drug Discov Today Dis Mech.* 2010;2:e135–e143. https://doi.org/10.1016/j.ddmec.2010.08.001
9. Cai L, Li W, Wang G, Guo L, Jiang Y, Kang YJ. Hyperglycemia-induced apoptosis in mouse myocardium: mitochondrial cytochrome C-mediated caspase-3 activation pathway. *Diabetes.* 2002;6:1938–1948. https://doi.org/10.2337/diabetes.51.6.1938
10. Guo CA, Guo S. Insulin receptor substrate signaling controls cardiac energy metabolism and heart failure. *J Endocrinol.* 2017;3:R131–r143. https://doi.org/10.1530/joe-16-0679
11. Zhang H, Ge S, He K, et al. FoxO1 inhibits autophagosome-lysosome fusion leading to endothelial autophagic-apoptosis in diabetes. *Cardiovasc Res.* 2019;14:2008–2020. https://doi.org/10.1093/cvr/cvz014
12. Zhang X, Tang N, Hadden T, Rishi A. Akt, FoxO and regulation of apoptosis. *Biochim Biophys Acta.* 2011;11:1978–1986. https://doi.org/10.1016/j.bbamcr.2011.03.010
13. Han Z, Truong Q, Park S, Breslow J. Two Hsp70 family members expressed in atherosclerotic lesions. *Proc Natl Acad Sci USA.* 2003;3:1256–1261. https://doi.org/10.1073/pnas.252764399
14. Zhang X, Chen X, Qi T, et al. HSPA12A is required for adipocyte differentiation and diet-induced obesity through a positive feedback regulation with PPARγ. *Cell Death Differen.* 2019;11:2253–2267. https://doi.org/10.1038/s41418-019-0300-2
15. Kong Q, Li N, Cheng H, et al. HSPA12A is a novel player in nonalcoholic steatohepatitis via promoting nuclear PKM2-mediated M1 macrophage polarization. *Diabetes.* 2019;2:361–376. https://doi.org/10.2337/db18-0035
16. Liu J, Du S, Kong Q, et al. HSPA12A attenuates lipopolysaccharide-induced liver injury through inhibiting caspase-11-mediated hepatocyte pyroptosis via PGC-1alpha-dependent acyloxyacyl hydrolase expression. *Cell Death Differ.* 2020;9:2651–2667. https://doi.org/10.1038/s41418-020-0536-x
17. Min X, Zhang X, Li Y, et al. HSPA12A unstabilizes CD147 to inhibit lactate export and migration in human renal cell carcinoma. *Theranostics.* 2020;19:8573–8590. https://doi.org/10.7150/thno.44321
18. Mao Y, Kong Q, Li R, et al. Heat shock protein A12A encodes a novel prosurvival pathway during ischaemic stroke. *Biochim Biophys Acta Mol Basis Dis.* 2018;5:1862–1872. https://doi.org/10.1016/j.bbadis.2018.03.006
19. Luo W, Lin K, Hua J, et al. Schisandrin B attenuates diabetic cardiomyopathy by targeting MyD88 and inhibiting MyD88-dependent inflammation. *Adv Sci.* 2022;31:e2202590. https://doi.org/10.1002/advs.202202590
20. Giacco F, Brownlee M. Oxidative stress and diabetic complications. *Circ Res.* 2010;9:1058–1070. https://doi.org/10.1161/circresaha.110.223545
21. Kannan S, Irwin M, Herbrich S, et al. Targeting the NRF2/HO-1 antioxidant pathway in FLT3-ITD-positive AML enhances

therapy efficacy. *Antioxidants*. 2022;11:717. https://doi.org/10.3390/antiox11040717
22. Dillmann W. Diabetic cardiomyopathy. *Circ Res*. 2019;8:1160–1162. https://doi.org/10.1161/circresaha.118.314665
23. Ke X, Chen J, Peng L, et al. Heat shock protein 90/Akt pathway participates in the cardioprotective effect of exogenous hydrogen sulfide against high glucose-induced injury to H9c2 cells. *Int J Mol Med*. 2017;4:1001–1010. https://doi.org/10.3892/ijmm.2017.2891
24. Li S, Liang M, Pan Y, et al. Exercise modulates heat shock protein 27 activity in diabetic cardiomyopathy. *Life Sci*. 2020;243:117251. https://doi.org/10.1016/j.lfs.2019.117251
25. Chen H, Shan Y, Yang T, et al. Insulin deficiency down-regulated heat shock protein 60 and IGF-1 receptor signaling in diabetic myocardium. *Diabetes*. 2005;1:175–181. https://doi.org/10.2337/diabetes.54.1.175
26. Shao S, Xiao L, Jia M, et al. Never in mitosis gene A-related kinase-6 deficiency deteriorates diabetic cardiomyopathy via regulating heat shock protein 72. *J Mol Med*. 2023;4:419–430. https://doi.org/10.1007/s00109-023-02295-7
27. Collins M, Clark MS, Truebano M. The environmental cellular stress response: the intertidal as a multistressor model. *Cell Stress Chaperones*. 2023;5:467–475. https://doi.org/10.1007/s12192-023-01348-7
28. Anon. Diagnosis and classification of diabetes mellitus. *Diabetes Care Suppl*. 2009;1:S62–S67. https://doi.org/10.2337/dc09-S062
29. Kenny HC, Abel ED. Heart failure in type 2 diabetes mellitus. *Circ Res*. 2019;1:121–141. https://doi.org/10.1161/circresaha.118.311371
30. Maahs DM, West NA, Lawrence JM, Mayer-Davis EJ. Epidemiology of type 1 diabetes. *Endocrinol Metab Clin N Am*. 2010;3:481–497. https://doi.org/10.1016/j.ecl.2010.05.011
31. Marino F, Salerno N, Scalise M, et al. Streptozotocin-induced type 1 and 2 diabetes mellitus mouse models show different functional, cellular and molecular patterns of diabetic cardiomyopathy. *Int J Mol Sci*. 2023;24:1132. https://doi.org/10.3390/ijms24021132
32. Teaney N, Cyr N. FoxO1 as a tissue-specific therapeutic target for type 2 diabetes. *Front Endocrinol*. 2023;14:1286838. https://doi.org/10.3389/fendo.2023.1286838
33. Zhang M, Sui W, Xing Y, et al. viaAngiotensin IV attenuates diabetic cardiomyopathy suppressing FoxO1-induced excessive autophagy, apoptosis and fibrosis. *Theranostics*. 2021;18:8624–8639. https://doi.org/10.7150/thno.48561
34. King A. The use of animal models in diabetes research. *Br J Pharmacol*. 2012;3:877–894. https://doi.org/10.1111/j.1476-5381.2012.01911.x
35. Li J, Zhang Y, Li C, et al. HSPA12B attenuates cardiac dysfunction and remodelling after myocardial infarction through an eNOS-dependent mechanism. *Cardiovasc Res*. 2013;4:674–684. https://doi.org/10.1093/cvr/cvt139
36. Wang Y, Liu J, Kong Q, et al. Cardiomyocyte-specific deficiency of HSPB1 worsens cardiac dysfunction by activating NFkappaB-mediated leucocyte recruitment after myocardial infarction. *Cardiovasc Res*. 2019;1:154–167. https://doi.org/10.1093/cvr/cvy163
37. Zhang X, Min X, Li C, et al. Involvement of reductive stress in the cardiomyopathy in transgenic mice with cardiac-specific overexpression of heat shock protein 27. *Hypertension*. 2010;6:1412–1417. https://doi.org/10.1161/hypertensionaha.109.147066
38. Kumar S, Sitasawad S. N-acetylcysteine prevents glucose/glucose oxidase-induced oxidative stress, mitochondrial damage and apoptosis in H9c2 cells. *Life Sci*. 2009;84:328–336. https://doi.org/10.1016/j.lfs.2008.12.016
39. Yao Y, Li R, Ma Y, et al. α-Lipoic acid increases tolerance of cardiomyoblasts to glucose/glucose oxidase-induced injury via ROS-dependent ERK1/2 activation. *Biochim Biophys Acta*. 2012;4:920–929. https://doi.org/10.1016/j.bbamcr.2012.02.005